Mineralium Deposita (2022) 57:1499–1514
https://doi.org/10.1007/s00126-022-01121-3

ARTICLE

Detrital zircon ages from Archaean conglomerates in the Singhbhum Craton, eastern India: implications on economic Au-U potential

Hartwig E. Frimmel[1,2] · Rajarshi Chakravarti[3,4] · Miguel A. S. Basei[5]

Received: 14 October 2021 / Accepted: 2 May 2022 / Published online: 17 May 2022

Abstract

New U–Pb age and Hf isotope data obtained on detrital zircon grains from Au- and U-bearing Archaean quartz-pebble conglomerates in the Singhbhum Craton, eastern India, specifically the Upper Iron Ore Group in the Badampahar Greenstone Belt and the Phuljhari Formation below the Dhanjori Group provide insights into the zircon provenance and maximum age of sediment deposition. The most concordant, least disturbed $^{207}Pb/^{206}Pb$ ages cover the entire range of known magmatic and higher grade metamorphic events in the craton from 3.48 to 3.06 Ga and show a broad maximum between 3.38 and 3.18 Ga. This overlap is also mimicked by Lu–Hf isotope analyses, which returned a wide range in $\varepsilon_{Hf}(t)$ values from + 6 to − 5, in agreement with the range known from zircon grains in igneous and metamorphic rocks in the Singhbhum Craton. A smaller but distinct age peak centred at 3.06 Ga corresponds to the age of the last major magmatic intrusive event, the emplacement of the Mayurbhanj Granite and associated gabbro, picrite and anorthosite. Thus, these intrusive rocks must form a basement rather than being intrusive into the studied conglomerates as previously interpreted. The corresponding detrital zircon grains all have a subchondritic Hf isotopic composition. The youngest reliable zircon ages of 3.03 Ga in the case of the basal Upper Iron Ore Group in the east of the craton and 3.00 Ga for the Phuljhari Formation set an upper limit on the age of conglomerate sedimentation. Previously published detrital zircon age data from similarly Au-bearing conglomerates in the Mahagiri Quartzite in the Upper Iron Ore Group in the south of the craton gave a somewhat younger maximum age of sedimentation of 2.91 Ga. There, the lower limit on sedimentation is given by an intrusive relationship with a c. 2.8 Ga granite. The time window thus defined for conglomerate deposition on the Singhbhum Craton is almost identical to the age span established for the, in places, Au- and U-rich conglomerates in the Kaapvaal Craton of South Africa: the 2.98–2.78 Ga Dominion Group and Witwatersrand Supergroup in South Africa. Since the recognition of first major concentration of gold on Earth's surface by microbial activity having taken place at around 2.9 Ga, independent of the nature of the hinterland, the above similarity in age substantially increases the potential for discovering Witwatersrand-type gold and/or uranium deposits on the Singhbhum Craton. Further age constraints are needed there, however, to distinguish between supposedly less fertile (with respect to Au) > 2.9 Ga and more fertile < 2.9 Ga successions.

Keywords Quartz-pebble conglomerate · Gold · Mesoarchaean · Singhbhum Craton · Zircon geochronology

Editorial handling: B. Lehmann

✉ Hartwig E. Frimmel
hartwig.frimmel@uni-wuerzburg.de

Rajarshi Chakravarti
rajarshi.chakravarti@es.iitr.ac.in

Miguel A. S. Basei
baseimas@usp.br

[1] Department of Geodynamics and Geomaterials Research, Institute of Geography and Geology, University of Würzburg, Am Hubland, 97074 Würzburg, Germany

[2] Department of Geological Sciences, University of Cape Town, Rondebosch 7700, South Africa

[3] Department of Applied Geology, Indian Institute of Technology (Indian School of Mines), Dhanbad, India

[4] Department of Earth Sciences, Indian Institute of Technology, Roorkee, India

[5] Instituto de Geociências, Universidade de São Paulo, São Paulo, Brazil

Introduction

For decades, Archaean conglomerates have been the focus of attention by academics as well as exploration companies because of their specific detrital mineral assemblage, that is, detrital pyrite, uraninite and, in places, gold, as well as their local association with carbon-rich material, perceived by many as relics of very early life forms. Such conglomerates are known from all continents (except Antarctica) and several of them gained fame for their endowment in gold and/or uranium minerals as exemplified by the world's largest known accumulation of gold in Mesoarchaean conglomerates of the Witwatersrand Basin in South Africa. Over more than a century of mining there, these conglomerates yielded a total of > 53,000 metric tons (t) of gold (Frimmel and Nwaila 2020), which is approximately 26% of all gold ever mined. Mining there left behind almost 1 Mt U_3O_8 in various waste tailings and > 200 kt U_3O_8 remain as resource in some of the conglomerates (Frimmel 2019). Gold enrichment of Archaean conglomerates has been ascribed to initial microbial gold fixation by possibly early photosynthesizing cyanobacteria in fluvial and littoral environments and subsequent mechanical reworking of such gold-bearing microbial mats to form rich placer deposits (Horscroft et al. 2011; Frimmel 2014, 2018; Heinrich 2015), although opposing views postulating an entirely hydrothermal origin are also debated (e.g. Fuchs et al. 2021). The enrichment in uranium is best explained by the preservation of detrital uraninite grains under an essentially oxygen-free Archaean atmosphere (Frimmel 2005; Burron et al. 2018) — a condition that lasted until the Great Oxidation Event (GOE) at around 2.3 Ga (e.g. Luo et al. 2016). Not surprisingly, conglomerates younger than the GOE are typically devoid of detrital uraninite. The same applies to detrital pyrite, which is highly abundant in fluvial conglomerates older than the GOE (Frimmel 2014).

The Singhbhum Craton in eastern India (Fig. 1) is one of the oldest know preserved land masses with a protracted record of sedimentation and magmatism from the Palaeoarchaean to the Neoproterozoic (e.g. Olierook et al. 2019; Prakash Pandey et al. 2019). Several Archaean conglomerate units have been described from that craton, some of which with elevated gold and uranium tenors (Chakravarti et al. 2018). Their age remains, however, poorly constrained, thus hindering a proper assessment of their economic potential. The latter aspect builds upon the notion that syn-depositional concentration of gold by microbial fixation set in on a larger scale only at about 2.9 Ga (Frimmel 2018), in which case Palaeo- to early Mesoarchaean conglomerates would be of little economic significance for gold mining. First U–Pb isotope analyses of detrital zircon grains from one of these conglomerates by Sunilkumar et al. (1996) gave age data from 3.09 to 3.04 Ga but also younger ages from 2.74 to 2.10 Ga. Their preliminary data suffer, however, from discordance and Pb loss, and consequently, they cannot be regarded as reliable. Subsequent attempts to date one of the conglomerates at a single locality by Ghosh et al. (2019) only led to the recognition that it must be younger than 3.25 Ga.

This paper aims at further constraining the age of conglomerates in the Singhbhum Craton by providing U–Pb age data on detrital zircon grains separated from key outcrops in two different geological positions: one in the Badampahar Greenstone Belt, where quartz-pebble conglomerate rests on top of the greenschist-facies metamorphosed volcano-sedimentary Palaeo- to Mesoarchaean Lower Iron Ore Group and forms the base of the Upper Iron Ore Group, whose age is unknown; and a second, representing the basal conglomerate of the Phuljhari Formation, which is stratigraphically between 3.38 and 3.25 Ga Singhbhum Suite granitoids and the Neoarchaean and/or Palaeoproterozoic Dhanjori Group.

Regional geological framework

The Singhbhum Craton comprises an old Palaeo- to Mesoarchaean basement that is overlain by Neoarchaean to Palaeoproterozoic volcano-sedimentary rocks of the Dhanjori, Simlipal and Malangtoli basins (Fig. 1). A central granitic to gneissic domain consists of two major lithostratigraphic units: (i) the 3.53–3.32 Ga tonalitic-trondhjemitic-granodioritic (TTG) Champua Suite (Upadhyay et al. 2014; Mitra et al. 2019; Olierook et al. 2019), previously also referred to as the Older Metamorphic Tonalite Gneiss. The Champua Suite was not derived from juvenile magmas but from recycled older continental crust as evidenced by Hadean zircon xenocrysts as old as 4240 Ma and zircon Hf isotope data (Chaudhuri et al. 2018); (ii) regionally more extensive granite and trondhjemite plutons, collectively referred to as the Singhbhum Suite, whose age is constrained between 3.38 and 3.25 Ga (Dey et al. 2020). This includes the 3.308 Ga Nilgiri Granite (Dey et al. 2017). The Singhbhum Suite plutons contain enclaves of, or are fringed by, older supracrustal rocks, consisting of micaschist, calc-silicate gneiss and amphibolite, lithostratigraphically unified as the Older Metamorphic Group. The youngest concordant age obtained on detrital zircon of 3375 ± 3 Ma (Nelson et al. 2014) constrains the maximum age of deposition of the Older Metamorphic Group, concordant U–Pb age of 3317 ± 8 Ma for metamorphic rutile (Upadhyay et al., 2014) its minimum age. Several episodes of regional metamorphism have been recognized: one prior to deposition of the Older Metamorphic Group at c. 3.37 Ga and then later-on at c. 3.32 and 3.26 Ga, evidenced by the above-mentioned rutile age and U–Pb data for metamorphic monazite (Prabhakar and Bhattacharya 2013;

see also Hofmann and Mazumder 2015). This was followed by regional peneplanation.

The central granite-gneiss domain is surrounded by low-grade metamorphic volcano-sedimentary greenstone belts that consist of phyllite, quartzite, metaconglomerates, carbonate rocks, chert, iron formation and intercalated mafic and felsic metavolcanic rocks. All of these are lithostratigraphically unified as the Iron Ore Group and they crop out in three distinct basins: the Gorumahisani-Badampahar Basin in the eastern, the Jamda-Koira Basin in the northwestern and the Tomka-Daiteri Basin in the southern part of the craton (Fig. 1). The age of the Iron Ore Group is only poorly constrained between at least 3.51 and 3.29 Ga. The upper age limit is given by a U–Pb zircon age of 3507 ± 2 Ma obtained on dacite from the Tomka-Daitari Basin (Mukhopadhyay et al. 2008). The youngest age available for the Iron Ore Group is a U–Pb zircon age of c. 3.29 Ga obtained on acid volcanic rocks in the Jamda-Koira Basin (Basu et al. 2008), which could be the volcanic equivalent of contemporaneous granite bodies of the Singhbhum Suite.

Based on recent field and geochronological studies, Saha et al. (2021) suggested a division of the eastern Iron Ore Group in the Gorumahisani-Badampahar Belt into an upper and lower sequence, separated by an unconformable contact. Low-grade metamorphosed komatiite, pillowed to massive metabasalts, tremolite-actinolite schist, banded iron formation, minor chert and banded quartzite constitute the lower sequence, whereas the upper sequence commences with a basal quartzpebble metaconglomerate, followed by massive quartzite, phyllite and mafic metavolcanic rocks. Zircon U–Pb analysis from a metakomatiite in the lower sequence yielded a $^{207}Pb/^{206}Pb$ age of 3340 Ma (Bachhar et al. 2021) but the truncated and resorbed boundaries of the zircon grains suggest that these are xenocrysts, probably inherited from the Singhbhum Suite. A biotite monzogranite of the Singhbhum Suite in this area contains enclaves of banded

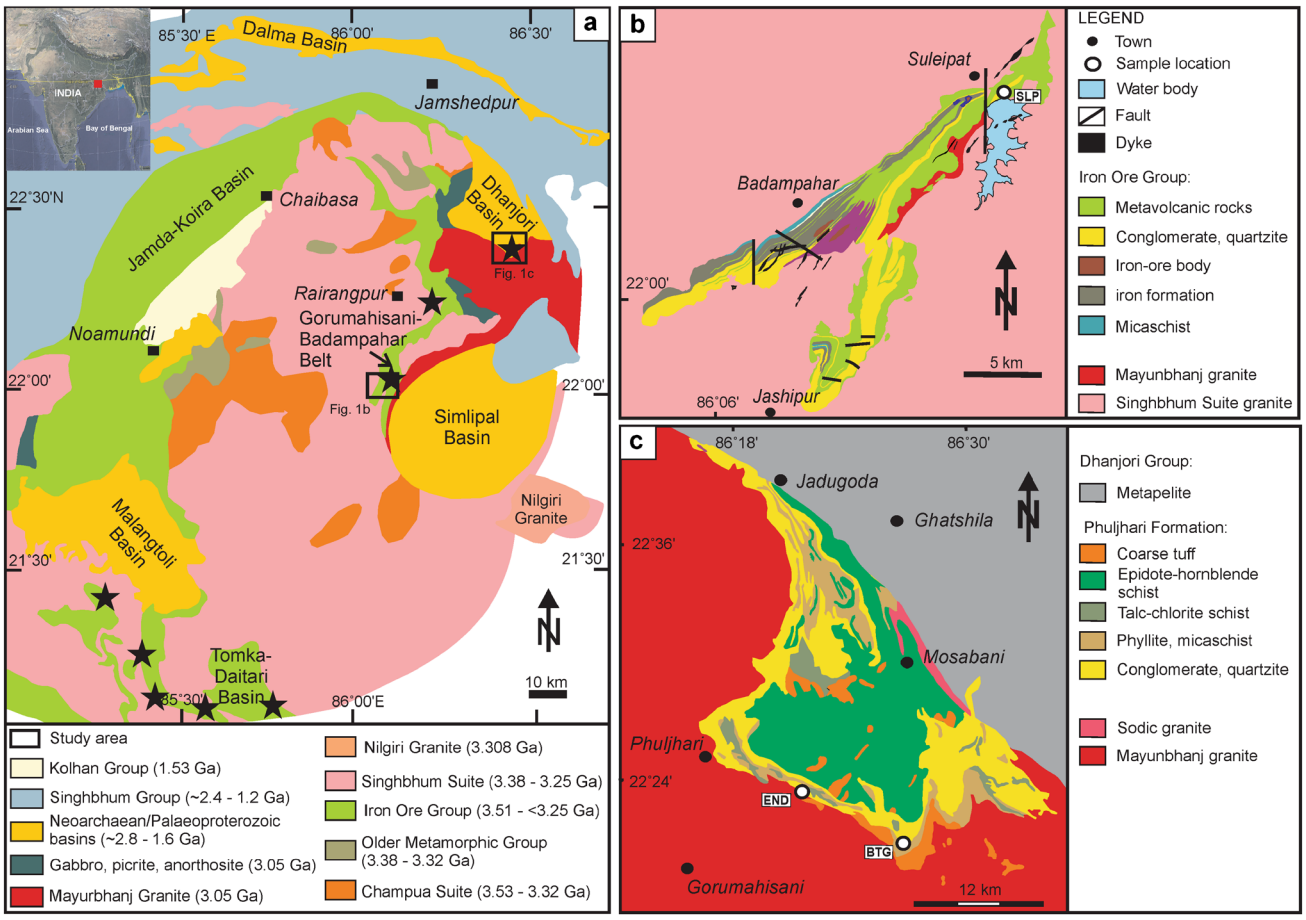

Fig. 1 **a** Regional geological map of the Singhbhum Craton; study areas shown as rectangles, stars indicate palaeoplacer gold occurrence (based on own observations and unpubl. data by edGeo Resources Pvt. Ltd. 2014); **b** geological map of the Badampahar Greenstone Belt (after Ghosh and Baidya 2017) with sample location; **c** geological map of the area east of Phuljhari (modified after Acharyya et al. 2010) with sample locations in the Phuljari Formation

iron formation and calc-silicate rocks, presumably of the lower sequence, as mapped by Saha (1994); a U–Pb zircon age of 3326 ± 5 Ma obtained on this monzogranite (Nelson et al. 2014) thus sets a minimum constraint on the age of the Lower Iron Ore Group. The age of the upper sequence, the Upper Iron Ore Group, is not well constrained. The youngest detrital zircon age obtained from a local conglomerate outcrop is 3250 Ma (Ghosh et al. 2019), which suggests a hiatus between the lower and upper sequence of > 70 million years. Consequently, whereas the Singhbhum Suite was intrusive into the Lower Iron Ore Group, it must have formed the basement for the Upper Iron Ore Group as already suspected by Roy and Bhattacharya (2012).

The above stratigraphic units are overlain by a package of Neoarchaean and/or Palaeoproterozoic volcano-sedimentary rocks in the Dhanjori, Simlipal and Malangtoli basins (Fig. 1). Deposition of the respective basin fills was probably not coeval. At the bottom of the Dhanjori Basin, an infra-Dhanjori unit, the Phuljhari Formation, should be Mesoarchaean in age because of an alleged intrusive relationship with an A-type potassic granite, the Mayurbhanj Granite and associated gabbro, picrite and anorthosite. The best available age for this phase of anorogenic magmatism is 3047 ± 17 Ma (Manikyamba et al. 2020). Consequently, the Phuljhari Formation should be older, seemingly confirmed by the above mentioned, imprecise preliminary detrital zircon age reported by Sunilkumar et al. (1996). Similarly, the basal siliciclastic succession of the adjacent Simlipal Basin yielded detrital zircon ages, the youngest of which is c. 3080 Ma (Bhattacharjee et al. 2021).

The bulk of the predominantly volcanic, subordinately fluvial and lacustrine fill of the intracontinental Dhanjori Basin, the Dhanjori Group is, however, considered to be distinctly younger, probably Neoarchaean and/or Palaeoproterozoic in age, though precise ages are not available (see review by Mukhopadhyay and Matin 2020).

Geological setting of the conglomerates

Badampahar Greenstone Belt

The eastern portion of the Iron Ore Group is exposed in the Badampahar Greenstone Belt (Fig. 1), where it comprises interbedded metavolcanic rocks, metaconglomerate, quartzite, metamorphosed iron formation, chert and schists, with minor metavolcaniclastic rocks. Metamorphic overprint reached lower amphibolite facies (Ghosh and Baidya 2017). The studied metaconglomerate rests with a tectonic contact upon a metakomatiite and grades upwards into quartzite, which, in turn, is overlain by metavolcanic rocks and iron formation. The metaconglomerate of interest here forms the basal unit of the Upper Iron Ore Group and is underlain by Singhbhum Suite granitoids, which, in turn, are intrusive into the Lower Iron Ore Group (see above). Gold nuggets of as much as 31.1 g in weight have been recovered from this conglomerate unit (Geological Survey of India, 2012), and artisanal mining activities document its economic potential.

Two samples (SLP-1 and SLP-2) were selected from a suite of samples taken from a section along the Suleipat dam (22° 8′35.62″ N, 86°14′14.23″ E) based on their relatively low degree of alteration and lack of quartz veins. The locality is of interest also because of reports of elevated Au contents, reaching as much as 2 g/t (Sarangi and Mohanty 1987). A detailed petrographic description and data on pyrite chemistry have been provided by Chakravarti et al. (2018). The sampled quartz-pebble conglomerate is largely clast-supported, with < 10 vol.% sand-sized quartz-rich matrix, although matrix-supported conglomerate is also common at the studied site (Fig. 2a and b). The total thickness of the conglomeratic unit varies from 5 to 85 m with individual conglomerate beds having a thickness of up to 1 m. A lack of sorting (clast size varies from 0.5 to 8 cm), absence of internal sedimentary structures, absence of preferred clast orientation (Fig. 2a and b) and an overall massive sheet-like geometry hint towards a debris-flow origin. The subrounded to rounded clasts of the overall oligomictic conglomerate consist predominantly of white vein quartz, chert and quartzite. In addition, some fuchsite-quartzite pebbles are also present. Detrital heavy minerals comprise zircon, monazite, chromite, pyrite and uraninite. The metamorphic matrix is made up of recrystallized quartz, chlorite and muscovite, suggesting a primary matrix consisting essentially of detrital quartz, illite and smectite.

Phuljhari Formation

The Phuljhari Formation is a sedimentary unit nonconformably overlying the Singhbhum Suite and, in turn, is unconformably overlain by mafic volcanic rocks of the presumably Neoarchean Lower Dhanjori Group (Acharyya et al. 2010). It consists of a basal metaconglomerate and intercalated quartzite, followed by purple phyllite, acid metavolcanic rocks, acid and basic metatuffs as well as mafic to ultramafic rocks metamorphosed at greenschist-facies conditions. Trough and tabular-cross bedding (online supplementary material Fig. SM1a and b), graded bedding and current ripples have been noted in the quartzite. Wave-generated structures and desiccation cracks are notably absent (Mazumder et al. 2019). Recent studies have revealed that the basal fluvial conglomerate-quartzite succession grades upward into thick mature quartz arenite, possibly of shallow shelf-origin (Yadav and Das 2021).

In many places, the lower contact of the formation is obscured by the 3.09–3.05 Ga Mayurbhanj Granite. Field

Fig. 2 Outcrop photographs of studied conglomerates: **a and b** base of the Upper Iron Ore Group in the Badampahar Greenstone Belt at the Suleipat dam: **a** unsorted, matrix-supported conglomerate, note deformed fuchsite quartzite clast (green) presumably derived from the lower Iron Ore Group; **b** unsorted boulder to cobble conglomerate; **c** basal Phuljhari Formation near Endrakati; and **d** basal Phuljhari Formation near Bhatgora

evidence as to the nature of this contact remains inconclusive, however, because it is unclear whether this granite is actually intrusive as alluded to by Acharyya et al. (2010) or forms the basement. During our field work, we could not observe any intrusive relationship.

Two localities were chosen for sampling, because previous bulk rock Au assays there had returned as much as 7 g/t (Haque and Dutta 1996). Furthermore, the locality has been known for years to contain elevated U concentrations due to up to 0.2 mm-sized rounded uraninite grains (Rao et al. 1988). Although on weathered surfaces not easily discernible, the metaconglomerate is, in its less weathered state, rich in pyrite, whereby both detrital pyrite and post-depositional pyrite generations can be distinguished. For detailed petrographic descriptions and pyrite chemical data, see Chakravarti et al. (2018).

One of the studied samples (END) was collected near the village Endrakati (22°24′6.55″ N, 86°18′30.48″ E), where a matrix-supported, oligomictic quartz-pebble conglomerate forms laterally discontinuous lenses 5 to 20 m in thickness. The clasts are rounded to sub-rounded, of elliptical shape, exhibit moderate sorting and in many instances display bedding-parallel orientation (Fig. 2c). The clast lithology is dominated by smoky and white vein quartz as well as quartzite. The size of quartzite clasts varies between 1 and 4 cm and that of the smoky and white quartz pebbles from 0.4 to 2 cm. Detrital heavy minerals observed are, in decreasing order of abundance, zircon, rutile, chromite, magnetite, pyrite, monazite and uraninite. The low-grade metamorphic matrix consists of recrystallized quartz, chlorite, fine-grained, in places fuchsitic, muscovite in the form of sericite.

The second sample locality (sample BTG) is near the village of Bhatgora (22°21′40.20″ N, 86°17′7.40″ E). There, a matrix-supported, oligomictic quartz-pebble conglomerate forms a lens c. 20 m in thickness and with a massive, sheet-like geometry. The rounded to subrounded clasts, mainly of vein quartz and quartzite, exhibit moderate sorting and no preferred orientation (Fig. 2d). Detrital heavy minerals are, in decreasing order of abundance, zircon, chromite, rutile, pyrite, monazite and uraninite. The metamorphic matrix is dominated by recrystallized quartz, chlorite, fuchsite (which gives the rock a dark green appearance in hand specimen) and minor fine-grained muscovite (sericite).

Methodology

Zircon grains were separated from each sample by conventional heavy mineral separation techniques and final hand-picking under a microscope. They were then mounted in epoxy, grinded down to reveal the centre of the grains and polished to a high finish. Transmitted light, cathodoluminescence and backscatter electron beam images helped to avoid grains with fractures and inclusions (for examples of images, see Fig. 3). Finally, 120 grains were selected from each sample (except for SLP1, which did not yield as many zircon grains) for isotope analysis.

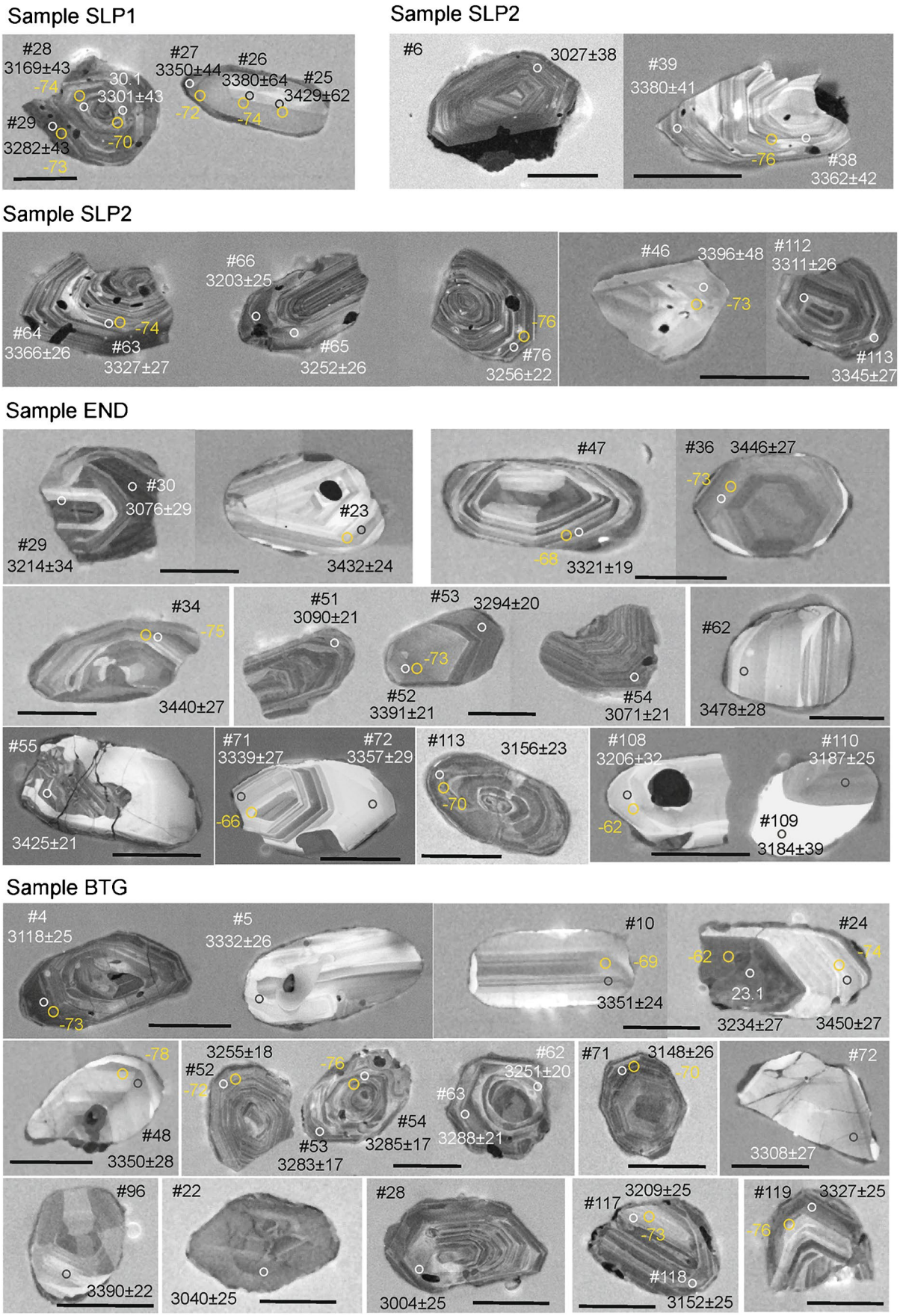
Sample SLP1
#28
3169±43
-74
30.1
3301±43
#27
3350±44
#26
3380±64
#25
3429±62
-72
-74
#29
-70
3282±43
-73
Sample SLP2
#6
3027±38
#39
3380±41
-76
#38
3362±42
Sample SLP2
#64
3366±26
-74
#63
3327±27
#66
3203±25
#65
3252±26
-76
#76
3256±22
#46
3396±48
#112
3311±26
-73
#113
3345±27
Sample END
#30
3076±29
#29
3214±34
#23
3432±24
#47
-68
3321±19
#36
3446±27
-73
#34
-75
3440±27
#51
3090±21
#53
3294±20
-73
#52
3391±21
#54
3071±21
#62
3478±28
#55
3425±21
#71
3339±27
#72
3357±29
-66
#113
3156±23
-70
#108
3206±32
#110
3187±25
-62
#109
3184±39
Sample BTG
#4
3118±25
-73
#5
3332±26
#10
-69
3351±24
#24
-62
-74
23.1
3234±27
3450±27
-78
#48
3350±28
3255±18
#52
-72
-76
#53
3283±17
#54
3285±17
#62
3251±20
#63
3288±21
#71
3148±26
-70
#72
3308±27
#96
3390±22
#22
3040±25
#28
3004±25
#117
3209±25
-73
#118
3152±25
#119
3327±25
-76

◂**Fig. 3** Examples of probed zircon grains under cathodoluminescence from samples SLP1, SLP2, END and BTG; spot numbers (#) refer to those in online supplementary Tables SM1, 2, 3 and 4. The given ages with 1 σ errors refer to the calculated $^{207}Pb/^{206}Pb$ age, spots analysed for their Lu–Hf isotopic composition are shown in yellow circles with corresponding $\varepsilon_{Hf}(0)$ values. Scale bars correspond to 100 µm

The in situ U–Pb analyses were carried out at the Geochronology Research Centre of the Instituto de Geociências, Universidade de São Paulo, Brazil, on a Thermo Fisher Scientific's multicollector inductively coupled plasma mass spectrometer (ICP-MS). Each analysis comprised 40 sequential measurements (with approx. 1 s integration time for each) in this Neptune machine, 10 with the ablating laser turned off (to obtain the instrumental blank) and the next 30 under the ablation of the Analyte Excite excimer laser on a 20 µm spot at the frequency of 6 Hz and intensity of 7 mJ. The ablated material was carried out by Ar (0.7 l/min) and He (0.6 l/min) gas flux. All isotope signals were simultaneously measured, four masses in Faraday cups (with greater amplitude): 206, 208, 232 and 238, and the other three in multiple ion counters due to their greater sensitivity: 202, 204 and 207. At the end of each measurement sequence, the mean instrumental blank value was immediately subtracted from each of the seven isotope signals. Note that the signal of mass 235 was not measured but mathematically obtained by dividing the signal of mass 238 by the relative abundance: 238/235 (= 137.88). The potential contribution to the signal of mass 204 by Hg (from the carrier gas) was assessed by subtracting from it the quotient of the signal of mass 202 and the relative abundance: 202/204 (= 4.355). Using the mass ratios 206/238, 207/235 and 208/232 as age estimates and the Stacey-Kramers formulae, the age-variable mass ratios of 206/204, 207/204 and 208/204 were calculated and the non-radiogenic Pb fraction ("common Pb") for the masses 206, 207 and 208 was then calculated by subtracting from each one the signal of mass 204 multiplied by the respective relative abundance (or mass ratio): 206/204, 207/204 and 208/204 previously calculated. Analyses of the GJ-1 standard were periodically repeated (approx. every 10 min) in order to compensate for errors and/or instrument drift in the subsequent samples. Tabulated and measured values for this GJ-1 standard provided the coefficients used to convert the total signals for $^{204}Pb + ^{206}Pb + ^{207}Pb + ^{208}Pb$, ^{232}Th and $^{235}U + ^{238}U$ into concentrations (in ppm), and also the fractionation correction factors of the mass ratios 206/238, 207/235, 207/206 and 208/232, before these were finally used to calculate the respective ages. During the period in which the analyses were performed, the standard 91,500 (Wiedenbeck et al. 1995) — with a reference age of 1065 Ma — was periodically measured as an unknown sample and yielded an age of 1066 ± 8 Ma.

Final data reduction was performed using Isoplot (Ludwig 2003). Analyses with common Pb content over 6% and discordance over 10% albeit listed in the data tables given (online supplementary material Tables SM1, 2, 3 and 4) were not used for further age interpretation. As all analysed zircon grains are distinctly older than 1300 Ma, $^{207}Pb/^{206}Pb$ ages are given preference over $^{206}Pb/^{238}U$ ages for the interpretation. Errors for the calculated ages are given at the 1 sigma level. The detrital age distribution modelling by probability density was performed using the kernel density estimation (Vermeesch 2012).

Using the same instrument pair (Neptune & Excite), in situ Lu–Hf isotope analyses were conducted on the same zircon domains that had been previously ablated for the U–Pb isotope analyses, in places having approximately the same CL response, and which had yielded relatively concordant U–Pb data. The size of the excimer laser beam was increased to 35 µm, its frequency to 7 Hz and its intensity reduced to 6 mJ. Using only Faraday cups, the following eight masses were simultaneously measured: 172, 173, 174, 175, 176, 177, 178 and 180. At the end of each measuring sequence, the mean instrumental blank was immediately subtracted from every isotopic signal. Abundance values published by IUPAC (https://ciaaw.org/pubs/TICE-2009.pdf) were then used to calculate the isotopic ratios between the Yb (172, 173, 174 and 176), Lu (175 and 176) and Hf (176, 177, 178 and 180) signals. Signals for masses 177, 178 and 180 were used to calculate both the Hf component of signal 174 and the fractionation coefficient of Hf (βHf) using exponential law. Signals for masses 172, 173 and the Yb component of 174 were used to calculate the fractionation coefficient (mass bias) of Yb (βYb) also through exponential law. As Lu does not have enough isotopes to allow self-correction, the fractionation coefficient of Lu is assumed to be βLu = βHf. The $^{176}Hf/^{177}Hf$ ratio was then obtained after subtracting the two interferences ^{176}Yb (estimated via βYb) and ^{176}Lu (estimated via βLu) from the 176 total signal.

The GJ-1 and 91,500 reference standards were analysed repeatedly amidst with each sample set to assess the Lu–Hf isotope data obtained on the unknown samples. The mean $^{176}Hf/^{177}Hf$ ratio obtained for the GJ-1 standard was 0.282003 ± 0.000036 which is close to the ratio of 0.282015 ± 0.000025 reported by Liu et al. (2010), and the one obtained for the 91,500 standard was 0.28235 ± 0.00007, which is close to the value of 0.282306 ± 0.000006 given by Woodhead and Hergt (2005). All Lu–Hf isotopic results are reported here with 95% confidence (or 2 σ) limits.

Initial $^{176}Hf/^{177}Hf$ ratios ($^{176}Hf/^{177}Hf_{(t)}$) were calculated by "internal" fractionation correction (i.e. using their own isotopes) from the measured $^{176}Hf/^{177}Hf$ and $^{176}Lu/^{177}Hf$ isotope ratios assuming a ^{176}Lu decay constant of 1.865×10^{-11} year^{-1} (Scherer et al. 2001) and recalling the U–Pb age obtained for each grain. Then $\varepsilon_{Hf(t)}$ values

were calculated from the $^{176}Hf/^{177}Hf_{(t)}$ using CHUR(t) values derived from the present day CHUR $^{176}Hf/^{177}Hf$ of 0.282785 and $^{176}Lu/^{177}Hf$ of 0.0336 (Bouvier et al. 2008). Estimated two-stage model ages (T_{DM}) are based on the measured $^{176}Lu/^{177}Hf$ ratio from each spot (first stage = age of zircon), a $^{176}Lu/^{177}Hf$ value of 0.0113 (Rudnick and Gao 2005) for the average continental crust and an average present-day composition of $^{176}Lu/^{177}Hf = 0.0384$ and $^{176}Hf/^{177}Hf = 0.28314$ for the depleted mantle (Chauvel et al. 2008).

In addition to the above, whole rock analyses of 24 conglomerate samples were conducted by conventional X-ray fluorescence spectrometry using a Panalytical Magi X Pro PW 2440 WDXRFS at the Department of Atomic Energy, Hyderabad (for details see Kumar et al. (2017) and by inductively coupled plasma-emission spectrometry at Bureau Veritas Mineral Laboratories in Vancouver (see https://commodities.bureauveritas.com), with the aim of establishing the degree of chemical weathering based on the chemical index of alteration (CIA). The CIA is calculated as $Al_2O_3/(Al_2O_3 + CaO^* + Na_2O + K_2O) \times 100$, whereby only the CaO within the silicate fraction of the samples is taken into consideration. As none of our samples contain measurable amounts of carbonates and/or Ca-phosphate, no CaO correction was necessary.

Zircon isotope data

A total of 30 spot analyses were obtained on 30 zircon grains from Sample SLP1. Most of the data are marked by relatively high common Pb and/or high degree of discordance. In some instances, the data might suggest analytical problems and all of these are rejected (marked in grey in online supplementary material Table SM1), which leaves only five analyses for further age interpretation. Their $^{207}Pb/^{206}Pb$ ages are between 3169 and 3429 Ma with a statistically insignificant peak at 3320 Ma. The Th/U ratio of these grains is between 0.8 and 3.1 (on average 1.7).

From sample SLP2, a total of 120 spot analyses were conducted (online supplementary material Table SM2). The majority of analyses yielded results with < 10% discordance and only these are used for further interpretation. Their Th/U ratio varies between 0.6 and 3.7 (on average 1.9; Fig. 4a). As the sample locality for both SLP1 and SLP2 is the same, the more or less concordant data from both samples are plotted together in a histogram showing the distribution of $^{207}Pb/^{206}Pb$ ages (Fig. 5a). The most concordant ages cluster at peaks around 3.20, 3.25, 3.30 and 3.36 Ga. The oldest data are 3415 ± 24 Ma at 99% and 3429 ± 62 Ma at 98% concordance. One almost perfectly concordant (101% concordance) datum of 3027 ± 38 Ma is from a spot (#6, Table SM2, Fig. 3) that is marked by a lack of any measurable common Pb and with Th/U of 1.1 in a relatively euhedral zircon grain marked by oscillatory zonation typical of magmatic zircon. It most likely reflects a true age of the igneous source rock and is considered the best available constraint on the maximum age of sedimentation.

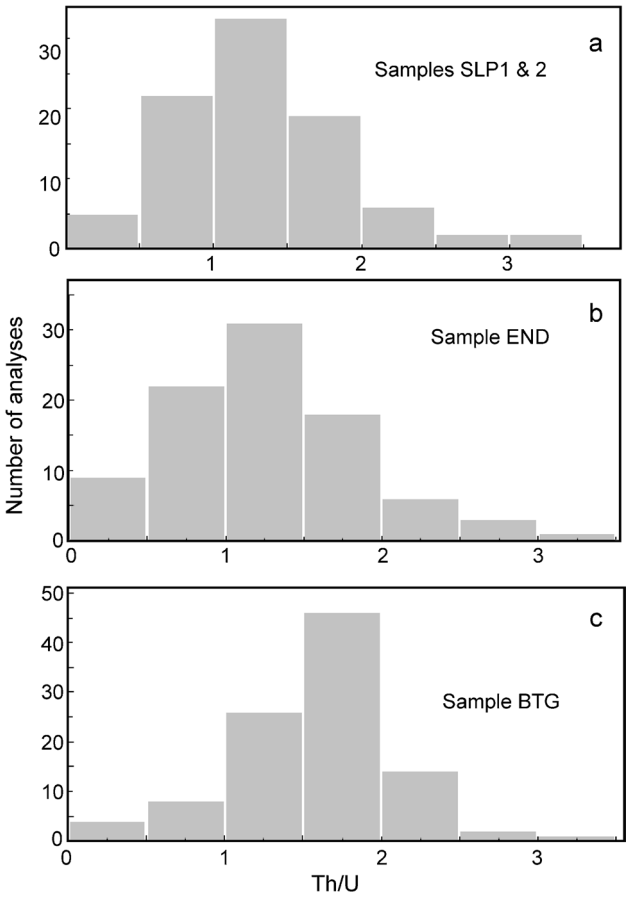

Fig. 4 Histograms of Th/U ratio in detrital zircon grains from **a** samples SLP1 and SLP2, **b** sample END, and **c** sample BTG

For the basal conglomerate samples END and BTG from the Phuljhari Formation, the zircon isotope data are presented in online supplementary material Tables SM3 and SM4, respectively. In each case, 120 spot analyses were conducted. For sample END, most analyses are relatively concordant (< 10% discordance) and those with high common Pb and/or highly discordant data are again omitted from further discussion. The distribution of calculated $^{207}Pb/^{206}Pb$ ages from relatively concordant data (Fig. 5b) reveals an abundance of ages at 3.14, 3.20 Ga, major peaks at 3.26 and 3.30–3.38 Ga and minor peaks at 3.43 and 3.48 Ga. The Th/U ratio of all acceptable analyses varies widely from 0.1 to 3.1 (one outlier at 21.6 probably reflects a different mineral and is discarded) with an average of 1.5 (Fig. 4b). The lowest age data obtained on almost perfectly concordant

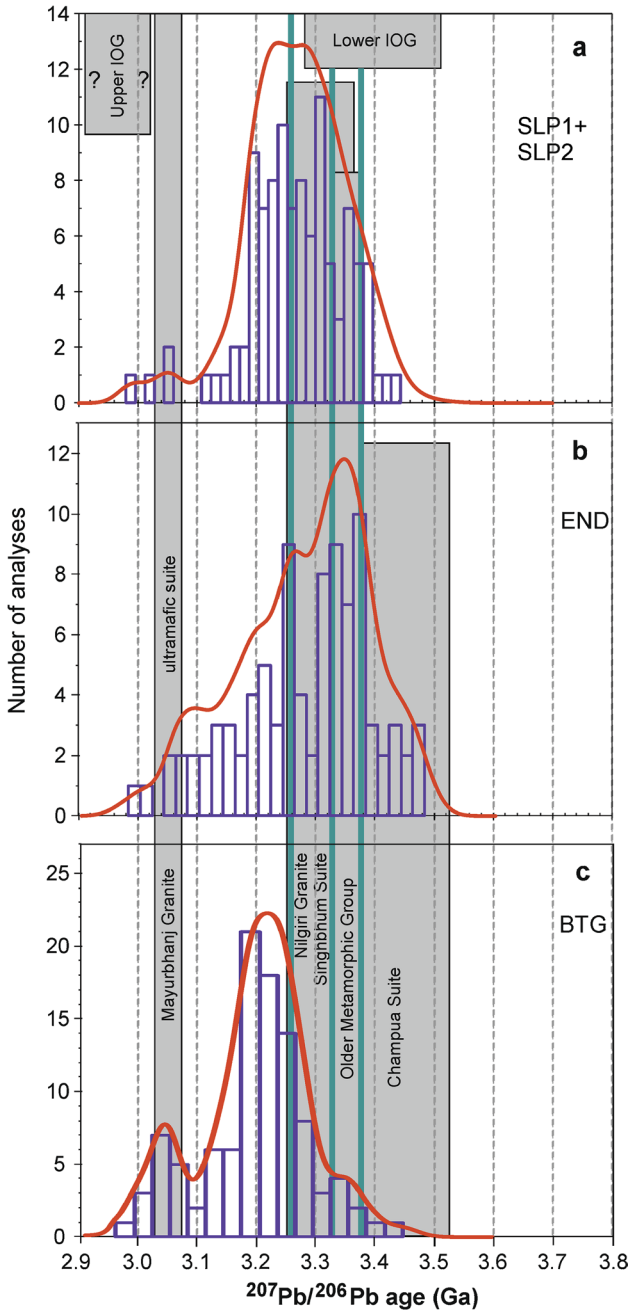

Fig. 5 Histograms showing the frequency distribution of relatively concordant $^{207}Pb/^{206}Pb$ ages obtained on detrital zircon grains: **a** samples SLP1 and SLP2, **b** sample END, **c** sample BTG. For reference, the age brackets for the major known magmatic (grey fields) and regional metamorphic (green lines) events in the Singhbhum Craton are also shown; IOG, Iron Ore Group

analyses and spots with < 1% common Pb (spots 54 and 30 in Table SM3) are 3071 ± 21 and 3076 ± 29 Ma. Spot 30.1 is from a zoned overgrowth with a Th/U of 0.7 over an older, oscillatorily zoned zircon core with Th/U of 0.7 (Fig. 3) without any evidence of significant alteration or Pb-loss. Similarly, spot 54 is from an oscillatorily zoned, evidently magmatic, zircon with Th/U of 0.7 that lacks signs of alteration or later Pb-loss. Both age data are taken as good approximation of the timing of zircon crystallization in the respective magmatic source rocks.

The age spectrum obtained for sample BTG looks slightly different (Fig. 5c). It displays a wide range of calculated $^{207}Pb/^{206}Pb$ ages from 2.73 to 3.45 Ga with a distinct main peak at 3.20 Ga and a minor peak at 3.03 Ga. The Th/U ratio of acceptable analyses is between 0.4 and 3.1, on average 1.6 (Fig. 4c). The oldest datum, 3450 ± 27 Ma, comes from a perfectly concordant analysis with no common Pb (spot 24 in Table SM4, Fig. 3) and is considered geologically meaningful. The youngest data from relatively concordant analyses are 3040 ± 25 Ma (spot 22 in Table SM4, 95% concordance) and 3004 ± 25 Ma (spot 28 in Table SM4, 109% concordance). They both lack common Pb, have a Th/U ratio of 1.6 and 1.4, respectively, and are perceived as representative of the age of the source rock and thus provide the best constraints on the maximum age of sedimentation.

Altogether, 82 zircon spots on domains that had yielded relatively concordant U–Pb data were analysed for their Lu–Hf isotopic composition (3 spots on two grains from sample SLP1, 27 in SLP2, 29 in END and 20 in BTG). For the full set of analyses, see online supplementary material Tables SM5, SM6, SM7, SM8. The $\varepsilon_{Hf}(t)$ values obtained for samples SLP1 and SLP2 are between − 4 and + 3.7 and between − 3 and + 6, respectively. The calculated t_{DM} for both sample sets is between 3.4 and 3.8 Ga, the $\varepsilon_{Hf}(t_{DM})$ between 3.9 and 5.3. In the case of sample END, the $\varepsilon_{Hf}(t)$ values range from − 1 to + 6, the calculated t_{DM} from 3.4 to 3.7 Ga, the $\varepsilon_{Hf}(t_{DM})$ from 4.0 to 5.9. For the zircon grains in sample BGT, the calculated $\varepsilon_{Hf}(t)$ values are with − 5 to + 1 somewhat lower, the calculated t_{DM} ages with 3.5 to 4.0 Ga and the $\varepsilon_{Hf}(t_{DM})$ with values from 3.2 to 4.7 similar.

Conglomerate geochemistry

Geochemical analyses of the matrix of 24 conglomerate samples (10 samples of the BTG sample locality, six from the END sample locality, four from the SLP sample locality and further four samples from a locality not used for zircon dating (BLB, from Baliabadi, 22°25′8.3″ N, 86°16′41.5″ E, also from the Phuljhari Formation) are presented in the online supplementary material Table SM9 with the aim of deciphering information on the degree of chemical weathering based on CIA values. Eight of these have a relatively low matrix proportion and complete physical separation of quartz-rich clasts could not be achieved. These have very high SiO_2 contents of > 96 wt.% and are not further considered for CIA calculations. The remaining analyses gave CIA values between 74 and 96, on average 82.

Discussion

The isotope data obtained on detrital zircon grains from the basal conglomerate of the Upper Iron Ore Group in the Badampahar Greenstone Belt and from the Phuljhari Formation at the base of the Dhanjori Basin make it possible to set some constraints on the maximum age of auriferous conglomerate deposition as well as on the zircon provenance, but also to assess the economic potential of these conglomerates hosting placer Au (and/or U) deposits.

Maximum age of sedimentation

The youngest detrital zircon grain in the conglomerate samples from the Badampahar greenstone belt has an age of 3027 ± 38 Ma. Its oscillatory zonation under CL (Fig. 3) and Th/U of 1.1 attests a magmatic derivation. The high level of concordance (101%) and total lack of common Pb suggest no post-crystallization Pb-loss. Consequently, this age is taken as the closest approximation to the upper limit for the time of sedimentation of the basal conglomerate of the Upper Iron Ore Group. In the case of the Phuljhari Formation conglomerate, the youngest zircon ages obtained for sample BTG are 3040 ± 25 Ma and 3004 ± 25 Ma. The former datum suffers from some discordance (95% concordance) and some common Pb (10.9%, Table SM4); Thus it might be slightly younger than the true formation age. Similarly, the latter datum is marked by some reverse discordance (109% concordance). Very little common Pb (2.4%, Table SM4) hint at this age coming close to the true age of zircon crystallistaion. Its Th/U of 1.4 and oscillatory zonation under CL (Fig. 3) speak for a magmatic origin. The youngest detrital zircon age obtained for sample END from the same formation is 3071 ± 21 Ma. It is based on a highly concordant analysis without any common Pb (Table SM3) and therefore regarded as representing the age of zircon crystallization. Its Th/U of 0.7 and oscillatory zonation under CL argue again for a magmatic origin. All in all, these data speak for conglomerate deposition at the base of the Phuljhari Formation at some time after 3.07 Ga, possibly even after 3.00 Ga.

Provenance

Based alone on clast lithology and the mineralogy of the detritus, a provenance of both granitic and mafic/ultramafic rocks, cross-cut by quartz veins, is indicated. Zircon, monazite and uraninite are likely derived from felsic sources, chromite and rutile from mafic/ultramafic ones. The vast majority of zircon grains in all analysed samples is characterized by Th/U ratios of > 0.5, which is commonly perceived as indicative of a magmatic origin (e.g. Kirkland et al. 2015). Previous studies have shown that Th/U of < 0.01 is typical of zircon that had crystallized from metamorphic fluids and Th/U of < 0.5 in metamorphically overprinted zircon (e.g. Zeh et al. 2010a,b). In the zircon populations analysed by us, only very few grains have Th/U of < 0.5, the vast majority is evidently of magmatic origin. No significant correlation exists between calculated age and Th/U (not shown). Noteworthy is, however, that the average Th/U in all our sample sets is markedly higher than that of magmatic zircon in other areas where it concentrates at values between 0.5 and 1.0. Reasons for variations in Th/U have been discussed inter alia by Kirkland et al. (2015), who contrasted the chemistry of zircon grains that crystallized under equilibrium conditions as opposed to fractionation in dependence on temperature. In general, zircon that formed in basic melts tends to have higher Th/U (> 1.5) than zircon from acidic melts (< 1.0), though a number of other parameters control zircon chemistry as shown for the Bushveld Complex in South Africa by Gudelius et al. (2020). The distribution of Th/U of zircon from the studied conglomerates (Fig. 4) suggests a mixture of felsic and mafic igneous source rocks with a higher proportion of mafic rocks in the source of the BTG conglomerate sample. The higher Th/U ratios obtained by us could be, however, also due to another variable, that is, reduced mobility of U under an oxygen-deficient Archaean atmosphere and, consequently, lower U contents in Archaean crust-derived magmas. This might be suggested by corresponding changes in whole-rock Th/U ratios in igneous rocks over time, specifically around the GOE and again in the Neoproterozoic (Liu et al. 2019).

Comparison with the known ages for magmatic and higher grade metamorphic events in the Singhbhum Craton reveals a good overlap with some of the peaks in detrital zircon ages, but some detrital zircon ages, especially the sub-peak at around 3.2 Ga, are apparently not reflected by the known magmatic and metamorphic events (Fig. 5). The detrital zircon ages span from 3.00 to 3.48 Ga, with a minor peak at 3.06, and a broad major peak between 3.18 and 3.39 Ga. Resolving individual sub-peaks within the latter gives maxima at around 3.20, 3.24, 3.30 and 3.35 Ga.

The older ages correspond well with those known from the Champua Suite and the roughly coeval Lower Iron Ore Group (Fig. 5). That age spectrum includes the Older Metamorphic Group. All three regional metamorphic events (green bars on Fig. 5) are mirrored by detrital zircon age peaks, especially in sample END from the Phuljhari Formation. The majority of detrital zircon ages (3.18–3.32 Ga) overlap with those for the Singhbhum Suite and the Lower Iron Ore Group both of which can be regarded as major source units. This is further supported by the Hf isotope data for the detrital zircon grains, which by and large overlap with published data on zircon from the Champua and Singhbhum suites as well as komatiite and, to a lesser extent, felsic volcaniclastic rocks from the Iron Ore Group (Fig. 6). Most

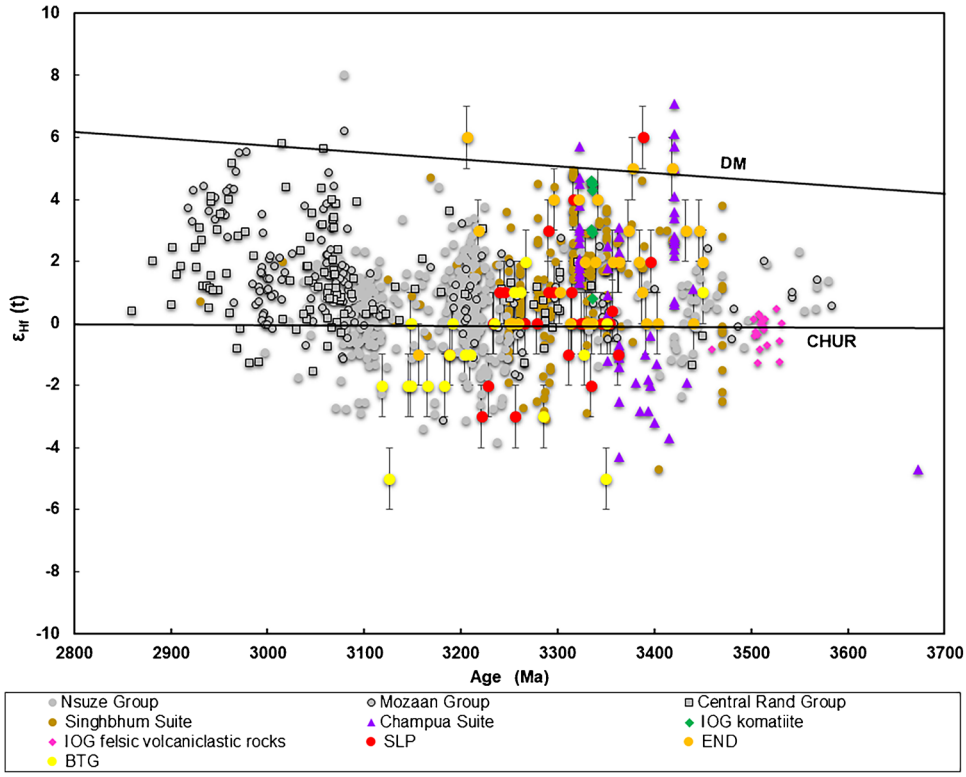

Fig. 6 ε_{Hf}(t) versus $^{207}Pb/^{206}Pb$ age plot for detrital zircon grains from samples SLP, END and BTG in comparison to published data for the Champua and Singhbhum suites (Dey et al. 2017; Mitra et al. 2019; Olierook et al. 2019; Prakash Pandey et al. 2019; Chaudhuri et al. 2018) and komatiite and felsic volcaniclastic rocks of the Iron Ore Group (Bachhar et al. 2021; Jodder et al. 2021); for comparison data for siliciclastic sedimentary rocks from the Central Rand Group of the Witwatersrand Supergroup (Koglin et al. 2010) and the Nsuze and Mozaan groups of the Pongoloa Supergroup (Wilson & Zeh 2018) are also shown

of these zircon grains have superchondritic ε_{Hf}(t) values indicative of magmatic crustal rocks derived from depleted mantle sources. Exceptions are some zircon grains from the Champua Suite with subchondritic ε_{Hf}(t) that points at recycling of pre-existing crust (Chaudhuri et al. 2018). The younger detrital zircon grains studied by us tend to have, on average, lower subchondritic ε_{Hf}(t) values, which suggests increased crustal recycling with decreasing age. Geological evidence of such a trend exists in the craton, e.g. in the form of anorogenic potassic granites with ages between 3079 ± 7 and 3115 ± 10 Ma (Chakraborti et al. 2019).

These A-type granite bodies, in the study area also known as Mayurbhanj Granite (Nelson et al. 2014), and probably related anorthosite, gabbro and picrite bodies, play a critical role in the assessment of the age of the studied conglomerate units. Zircon ages of 3123 ± 7, 3122 ± 5 and 3119 ± 6 Ma previously obtained for the gabbroic suite (Augé et al. 2003) probably reflect inheritance as indicated by the most recently obtained age of 3047 ± 17 Ma for a gabbro of this suite (Manikyamba et al. 2020). Zircon grains with corresponding ages are not the most common in the studied conglomerates but constitute a distinct sub-peak in the age histograms for both the Phuljhari Formation as well as the Upper Iron Ore Group (Fig. 5). This implies that the Mayurbhanj Granite was not intrusive into the studied conglomerates as previously perceived (e.g. Mukhopadhyay and Matin 2020) but must be older. Thus the age of the Mayurbhanj Granite can be used as a first-order constraint on the maximum age of sediment deposition. This granite, together with the associated mafic and ultramafic rocks, seemingly constituted an important source of the studied conglomerates. A dominance of the Mayurbhanj Granite in the sediment source area is further indicated by geochemical data on the matrix of the conglomerates. They show chondrite-normalized rare earth patterns that are identical to those of the Mayurbhanj Granite (Chakravarti 2020).

Comparison with other siliciclastic sequences on the Singhbhum Craton

The age range obtained on detrital zircon in this study is very similar to that previously reported for detrital zircon grains from the Keonjhar Quartzite, that is, 3585 to 3024 Ma (Mukhopadhyay et al. 2014), and the Mahagiri Quartzite. The latter term has been used to describe an up to 1500 m thick sequence of shelf-facies quartz arenite, conglomerate, mudstone and minor volcanic rocks, which rests unconformably on top of the southern Iron Ore Group with a palaeosol on that contact (Mukhopadhyay et al. 2014). Detrital zircon ages are mainly between 3510 and 3176 Ma (86% of data), with fewer ages of as low as 2909 ± 7 Ma (Sreenivas et al. 2019). The latter is based on 100% concordant data and thus provides the best constraint on the maximum age of sediment deposition. The youngest age obtained for detrital zircon in the Keonjhar Quartzite, 3024 ± 13 Ma, is in very good agreement with the youngest reasonably concordant

age obtained in our study. Interestingly, this quartzite unit is associated with a fluvial conglomerate that has been the target of numerous artisanal workings for placer gold. Our new data also compare well with detrital zircon ages from intracratonic modern river sands, 87% of which are in the range of 3.50 to 3.22 Ga, with minor populations at 3.62–3.55 Ga and at 3.10–3.06 Ga (Miller et al. 2018). The latter age peak is of particular interest because it is close to the youngest peak in our new data, which has been used above to argue for the Mayurbhanj Granite having been source of some detrital particles into the studied conglomerates rather than being intrusive into them.

Implications on palaeoplacer gold potential

With the realization that the global gold cycle started in earnest at around 2.9 Ga when microbes managed to fix large amounts of Au from meteoric (and possibly also shallow sea) water and thus formed the first gigantic gold deposits in Earth's history in the form of palaeoplacers (Frimmel 2018), the age of conglomerates on old cratons has become the probably most important parameter controlling their gold potential. The likelihood of such conglomerates hosting large gold placer deposits is not dictated anymore by the geological makeup of the hinterland as presumed in older literature (e.g. Frimmel et al. 2005) but by their age. The world's richest gold palaeoplacers in the Witwatersrand Basin in the Kaapvaal Craton of South Africa can be explained by leaching of background concentrations of Au from the Palaeo- to Mesoarchaean hinterland and the intermediate step of microbially induced precipitation of Au that was dissolved in the meteoric run-off from the old cratonic land surface (Frimmel 2014; Frimmel and Hennigh 2015; Heinrich 2015). This genetic model does not require any specific lithology in the hinterland as a gold source as illustrated by the world's richest gold deposits in the Witwatersrand (Nwaila et al. 2017). The distribution of gold in Archaean and Proterozoic placer deposits worldwide clearly shows a peak in sedimentary gold fixation by 2.9 Ga and an exponential decrease in Au endowment and grade from then onwards (Frimmel 2018). As this gold mega-event at 2.9 Ga was controlled by a combination of fortuitous circumstances in the evolution of the atmosphere, biosphere and geosphere, it must have been a global phenomenon on all Archaean cratons. The fact that the Kaapvaal Craton hosts one to two orders of magnitude more gold than other cratons — as far as known to date — is not due to some unexplained special gold concentrations mechanism there but is essentially a matter of preservation of such ancient sedimentary rocks. Consequently, the gold potential of the conglomerates in the Singhbhum Craton becomes a question of sediment age.

This study revealed that the age of the 3047 ± 17 Ma Mayurbhanj Granite and associated mafic to ultramafic rocks can be used as constraint on the maximum age of conglomerate deposition, both in the Upper Iron Ore Group and the Phuljhari Formation. The youngest relatively concordant detrital zircon ages of 3027 ± 38 Ma and 3004 ± 25 Ma, respectively, for these two units provide further limits. Identical upper limits on the age of deposition have been obtained for the Keonjhar Quartzite, whereas the Mahagiri Quartzite should be younger than 2909 ± 7 Ma. The minimum age of clastic sediment deposition remains elusive as no reliable age data exist for the overlying Dhanjori Group in the case of the Phuljhari Formation, nor for the Upper Iron Ore Group. The similarity in the detrital zircon age spectra between the studied conglomerates and the Mahagiri Quartzite (Sreenivas et al. 2019) could point to a similar depositional setting and roughly similar age. In the Mahagiri Range, c. 2.80 Ga granite was emplaced into this quartzite (Mukhopadhyay et al. 2014), thus setting a minimum on the age of the Mahagiri Quartzite. Thus, the Mahagiri Quartzite's age is perfectly within the "golden period" during which most of the Witwatersrand placer gold was deposited, that is, from 2.90 to 2.78 Ga — the age of the Central Rand Group. The potential exists that the basal conglomerates of the Upper Iron Ore Group and the Phuljhari Formation also have an age within this range, although they could also be slightly older.

From the Witwatersrand strata, we have learned that the gold placer potential in clastic deposits older than 2.9 Ga (such as in the 2.98–2.96 Ga Dominion Group and the overlying 2.96–2.90 West Rand Group, Paprika et al. 2021) is very low, in stark contrast to the highly auriferous 2.90–2.78 Ga deposits in the Central Rand Group. Conglomerates of similar age also occur in the upper Mozaan Group (Pongola Supergroup) in the eastern part of the Kaapvaal Craton and detrital zircon data suggest a similar source (Zeh and Wilson 2022). Some of them have been mined for gold in the past (Luskin et al. 2019), but the overall gold endowment is less and possibly related to a lack of Au-rich microbial mats in the respective hinterland, differences in depositional setting or possibly stronger mobilization of Au by metamorphic fluids leading to the formation of orogenic-type gold-quartz veins (Luskin et al. 2019).

Note that the concentration of Au and U, both in detrital heavy minerals (native gold and uraninite), was clearly decoupled from each other. The > 2.9 Ga conglomerates can be very rich in detrital uraninite, whose abundance was controlled mainly by the lack of oxygen in the contemporaneous atmosphere (Frimmel 2005). The possible reasons for the lack of gold in placers older than 2.9 Ga have been speculated upon as follows (Frimmel 2018): (i) a lack of microbes capable of trapping large amounts of gold, (ii) a lack of crustal abundance in Au due to modern-style plate tectonics not having operated yet and thus preventing the subduction factory to transfer and concentrate gold in

continental crustal rocks, and/or (iii) a lower Au concentration in surface waters due to lower degrees of weathering in an overall colder climate.

As for point (i), so far, no evidence of former microbial mats as documented for the 2.9 Ga lower Central Rand Group in the Witwatersrand Basin has been found in the Singhbhum Craton. Although Chakravarti et al. (2018) suggested the presence of microbial remnants in the studied conglomerates, the evidence of it remains problematic and the described morphological features of the carbonaceous material resemble those that have been identified as abiotic (Criouet et al. 2021). Maybe the local depositional environment was not suitable for the development of larger microbial communities. The hitherto only modest Au grades recognized in the conglomerates of the Singhbhum Craton may be also due to a lack of a sufficiently large redox potential on the surface of the microbial mats in order to trap large amounts of gold from meteoric waters. This would apply to anoxygenic photosynthesizers which, in all likelihood, preceded their oxygenic relatives. The transition from anoxygenic to oxygenic photosynthesis presumably took place gradually from about 3.0 Ga onwards (Planavsky et al. 2014) with evidence of at least locally oxygenated shallow oceans already in the Mesoarchaean (Eickmann et al. 2018). Conglomerates older than 2.9 Ga might, therefore, have less potential of hosting large amounts of gold.

As point (ii) concerns, a marked paucity of larger orogenic or porphyry gold deposits in rocks older than 2.8 Ga has been explained by a lack of modern-style subduction (Frimmel 2018). Subduction is seen as a critical prerequisite for the concentration of a number of metals (including Au) in the supra-subduction subcontinental lithospheric mantle wedge and the efficient transfer of these metals from this source region to upper crustal levels, where they could be further concentrated to form ore deposits. If this notion is correct, older Palaeoarchaean rocks should be less fertile than Neoarchaean ones.

Regarding point (iii), it can only be speculated upon based on palaeoclimate proxies, such as sediment deposits indicative of extreme climate conditions and geochemical evidence, such as chemical index of alteration (CIA) as proxy of chemical weathering intensity. In the Witwatersrand Basin, the chemistry of clastic sedimentary rocks in the gold-rich Central Rand Group are marked by relatively high CIA, deep chemical weathering profiles beneath erosional surfaces and a lack of detrital feldspar but omnipresence of pyrophyllite. These lithogeochemical and mineralogical characteristics have been explained by intense chemical weathering that led to widespread kaolinitization on the old erosion surfaces (Frimmel and Minter 2002). This is in stark contrast to far less weathered clastic rocks in the underlying West Rand Group, which is relatively poor in Au. By analogy, the studied conglomerates from the Singhbhum Craton are devoid of (detrital) feldspars and carbonates, which is indicative of relatively acidic conditions as can be expected under the Archaean atmosphere and also of elevated chemical weathering rates. This is also reflected by generally high chemical indices of alteration (CIA) between 74 and 91 obtained on the matrix of conglomerate samples from the localities studied in this project. Furthermore, evidence of elevated levels of chemical weathering in the Archaean hinterland of the Singhbhum Craton has been documented in siliciclastic rocks of similar age in the Jamda-Koira Basin (western IOG), the base of the Mahagiri Quartzite and the Keonjhar Quartzite (Mukhopadhyay et al. 2014; Ghosh et al. 2016; Kumar et al. 2017). Taking the Witwatersrand as reference, all of the above evidence of elevated chemical weathering rates would suggest a depositional age of < 2.9 Ga for the conglomerates in the Singhbhum Craton. This would speak for a high potential of finding Witwatersrand-type deposits there.

Much has been speculated upon the importance of source rocks for the gold endowment of the Witwatersrand conglomerates (e.g. Nwaila et al. 2017). If the placer model with initial derivation from mechanically reworked microbial mats (Frimmel 2014) is accepted, the lithology of the hinterland loses its metallogenic importance. More important seems to be, however, the tectonic setting of the depositional environment. This becomes evident from the distribution of the $\varepsilon_{Hf}(t)$ values. Whereas the largely chondritic Hf isotopic composition of the detrital zircon grains in the conglomerates from the Singhbhum Craton is similar to that of detrital zircon in conglomerate and sandstone units from the Kaapvaal Craton, the age distribution is different (Fig. 6). The gold-rich Central Rand Group is marked by relatively young detrital zircon ages much closer to the time of deposition, which is indicative of an active tectonic regime with uplift of the hinterland as can be expected in a foreland basin. This resulted in numerous low-angle unconformities within the basin fill, each of which made possible the reworking of underlying strata and thus the upgrading of placer deposits (e.g. Frimmel and Nwaila 2020). Such an effect is not indicated by the zircon isotope data for the conglomerates from the Singhbhum Craton, where a comparable large number of intra-group unconformities is, according to our current understanding, absent. This resulted also in an overall much lower thickness of the siliciclastic basin fill, which severely reduces the overall gold potential.

Conclusions

The new age data obtained for detrital zircon grains from gold- and, in places, U-bearing Archaean conglomerates set some constraints on the maximum age of sediment deposition, that is, < 3.03 Ga in the case of the basal

Upper Iron Ore Group in the Badampahar Greenstone Belt and < 3.00 Ga in the case of the Phuljhari Formation. For the Mahagiri Quartzite, previous age data suggest a maximum depositional age of 2.91 Ga (Sreenivas et al. 2019) and a minimum age of 2.8 Ga (Mukhopadhyay et al. 2014). This range corresponds almost perfectly with that of the Central Rand Group in the Witwatersrand Basin — the world's largest known reservoir of gold and one of the richest uranium provinces. By analogy with the Witwatersrand ore province, it can be concluded that, if the studied conglomerates are older than c. 2.9 Ga, they would have a significant U but only limited Au potential. If they are younger than c. 2.9 Ga, the potential exists not only for uranium but also for larger gold deposits. In order to assist further exploration initiatives in the region, it is recommended to assess the extent of Mesoarchaean palaeoweathering by conducting a lithogeochemical study on fresh (that is, unaffected by recent weathering) samples in addition to further efforts to set narrower constraints on the age of deposition. Any indication of intense weathering in the source and/or the depositional position of the conglomerates could then be used as encouragement for further exploration for Witwatersrand-type gold deposits. A significant drawback for the gold potential of the studied conglomerate units is, however, an overall lack of sediment thickness due to a lack of intrabasinal sediment reworking as can be expected in a foreland basin. This is indicated also by our new Hf isotope data. The chances of discovering gold deposits of the same scale as in the Witwatersrand are, therefore, considered slim but potential for smaller economic deposits does exist.

Moreover, our new isotope data show that effectively all Palaeo- and Mesoarchaean units known so far on the Singhbhum Craton contributed to the mix of detrital grains in the studied conglomerates. Zircon ages covering the entire spectrum from 3.5 to 3.1 Ga are present, with a main peak between 3.18 and 3.36 Ga, partly corresponding to the ages of the Champua Suite, the Singhbhum Suite, the Older Metamorphic Group and the Lower Iron Ore Group. This overlap is further supported by similar Hf isotopic compositions. A minor but distinct age peak at 3.06 Ga can be correlated to the age of the Mayurbhanj Granite and related ultramafic suite, which clearly acted as a significant source for the clastic components in the studied conglomerates and was not intrusive into the clastic sediment cover as previously assumed.

Last but not least, our new results confirm the recent suggestion of a division of the Iron Ore Group into a lower and upper sequence (Saha et al. 2021). Whereas a Palaeoarchaean age for the lower sequence is well established, the upper sequence turned out to be much younger than hitherto thought, that is, < 3.03 Ga. It is, in all likelihood, entirely unrelated to the lower sequence, which calls for a fundamental revision of the lithostratigraphic nomenclature for the Singhbhum Craton.

Supplementary Information The online version contains supplementary material available at https://doi.org/10.1007/s00126-022-01121-3.

Acknowledgements RC gratefully acknowledges a Junior Research Fellowship from IIT (ISM) Dhanbad. S Singh and A S Venkatesh are thanked for facilitating the zircon separation at the heavy mineral separation lab at the Department of Applied Geology at the same institution. We are grateful to FAPESP (Thematic Project 2015/03737-0), which made it possible to carry out the U-Pb isotope analyses. We thank A. Zeh and A. Hofmann for their very constructive reviews.

We herewith declare that we have no conflicts of interest or any competing interests to disclose. The analyses were funded through a FAPESP grant to MASB (Thematic Project 2015/03737-0).

Funding Open Access funding enabled and organized by Projekt DEAL.

References

Acharyya SK, Gupta A, Orihashi Y (2010) Neoarchean-Paleoproterozoic stratigraphy of the Dhanjori basin, Singhbhum Craton, Eastern India: and recording of a few U-Pb zircon dates from its basal part. J Asian Earth Sci 39:527–536

Augé T, Cocherie A, Genna A, Armstrong R, Guerrot C, Mukherjee MM, Patra RN (2003) Age of the Baula PGE mineralization (Orissa, India) and its implications concerning the Singhbhum Archaean nucleus. Precambr Res 121:85–101

Bachhar P, Saha D, Santosh M, Liu HD, Kwon S, Banerjee A, Patranabis-Deb S, Deb GK (2021) Mantle heterogeneity and crust-mantle interaction in the Singhbhum craton, India: new evidence from 3340 Ma komatiites. Lithos 382–383:105931

Basu AR, Bandyopadhyay PK, Chakraborti R, Zou H (2008) Large 3.4 Ga Algoma type BIF in the Eastern Indian Craton. Geochimica et Cosmochimica Acta 72:A59

Bhattacharjee S, Mulder J, Roy S, Chowdhury P, Cawood P, Nebel O (2021) Unravelling depositional setting, age and provenance of the Simlipal volcano-sedimentary complex, Singhbhum Craton: evidence for Hadean crust and Mesoarchean marginal marine sedimentation. Precambr Res 354:106038. https://doi.org/10.1016/j.precamres.2020.106038

Bouvier A, Vervoort JD, Patchett PJ (2008) The Lu–Hf and Sm–Nd isotopic composition of CHUR: constraints from unequilibrated chondrites and implications for the bulk composition of terrestrial planets. Earth Planet Sci Lett 273:48–57

Burron I, da Costa G, Sharpe R, Fayek M, Gauert C, Hofmann A (2018) 3.2 Ga detrital uraninite in the Witwatersrand Basin, South

Africa: evidence of a reducing Archean atmosphere. Geology 46:295–298
Chakraborti TM, Ray A, Deb GK, Upadhyay D, Chakrabarti R (2019) Evidence of crustal reworking in the Mesoarchean: insights from geochemical, U-Pb zircon and Nd isotopic study of a 3.08–3.12 Ga ferro-potassic granite-gneiss from north-eastern margin of Singhbhum Craton. India Lithos 330–331:16–34
Chakravarti R, Singh S, Venkatesh AS, Patel K, Sahoo PR (2018) A modified placer origin for refractory gold mineralization within the Archean radioactive quartz-pebble conglomerates from the eastern part of the Singhbhum Craton, India. Econ Geol 113:579–596
Chakravarti, R. (2020) Genesis of gold mineralization associated with Archean quartz-pebble-conglomerates (QPC) in and around the Eastern Iron Ore Group, Singhbhum Craton, eastern India. Unpubl PhD thesis, Indian Institute of Technology (Indian School of Mines), Dhanbad, India. 201 p
Chaudhuri T, Wan Y, Mazumder R, Ma M, Dunyi Liu D (2018) Evidence of enriched Hadean mantle reservoir from 4.2–4.0 Ga zircon xenocrysts from Palaeoarchean TTGs of the Singhbhum Craton, eastern India. Sci Rep 8:7069. https://doi.org/10.1038/s41598-018-25494-6
Chauvel C, Lewin E, Carpenter M, Arndt N, Marini J-C (2008) Role of recycled oceanic basalt and sediment in generating the Hf-Nd mantle array. Nat Geosci 1:64–67
Criouet I, Viennet J-C, Jacquemot P, Jaber M, Bernard S (2021) Abiotic formation of organic biomorphs under diagenetic conditions. Geochem Perspect Let 16:40–46
Dey S, Topno A, Liu Y, Zong K (2017) Generation and evolution of Palaeoarchaean continental crust in the central part of the Singhbhum craton, eastern India. Precambr Res 298:268–291
Dey S, Nayak S, Mitra A, Zong K, Liu Y (2020) Mechanism of Paleoarchean continental crust formation as archived in granitoids from northern part of Singhbhum Craton, eastern India. Geol Soc Lond Spec Publ 489:189–214
Eickmann B, Hofmann A, Wille M, Bui TH, Wing BA, Schoenberg R (2018) Isotopic evidence for oxygenated Mesoarchaean shallow oceans. Nat Geosci 11:133–138
Frimmel HE (2005) Archaean atmospheric evolution: evidence from the Witwatersrand gold fields, South Africa. Earth Sci Rev 70:1–46
Frimmel HE (2018) Episodic concentration of gold to ore grade through Earth's history. Earth-Sci Rev 180:148–158
Frimmel HE, Groves D, Kirk J, Ruiz J, Chesley J, Minter WEL (2005) The formation and preservation of the Witwatersrand Goldfields, the world's largest gold province. In: Hedenquist JW, Thompson JFH, Goldfarb RJ, Richards JP (eds) Economic Geology One Hundredth Anniversary Volume. Society of Economic Geologists, Littleton, pp 769–797
Frimmel HE (2014) A giant Mesoarchean crustal gold-enrichment episode: possible causes and consequences for exploration In: Kelley K, Golden HC (eds) Building exploration capability for the 21st century. Society of Economic Geologists, Special Publication 18, Littleton, pp 209–234
Frimmel HE (2019) The Witwatersrand Basin and its gold deposits In: Kröner A, Hofmann A (eds) The archaean geology of the Kaapvaal Craton. Southern Africa. Springer Nature, Cham, pp 255–275
Frimmel HE, Hennigh Q (2015) First whiffs of atmospheric oxygen triggered onset of crustal gold cycle. Mineralium Deposita 50:5–23
Frimmel HE, Minter WEL (2002) Recent developments concerning the geological history and genesis of the Witwatersrand gold deposits, South Africa. In: Goldfarb RJ, Nielsen RL (eds) Integrated methods for discovery: global exploration in the twenty-first century. Society of Economic Geologists Spec Publ 9, Littleton, pp 17–45
Frimmel HE, Nwaila GT (2020) Geologic evidence of syngenetic gold in the Witwatersrand goldfields, South Africa In: Sillitoe RH, Goldfarb RJ, Robert F, Simmons SF (eds) Geology of the world's major gold deposits and provinces. Society of Economic Geologists Spec Publ 23, Littleton, pp 645–668
Fuchs S, Schumann D, Martin RF, Couillard M (2021) The extensive hydrocarbon-mediated fixation of hydrothermal gold in the Witwatersrand Basin. Ore Geology Reviews in press, South Africa. https://doi.org/10.1016/j.oregeorev.2021.104313
Geological Survey of India (2012) Geology and mineral resources of Odisha: miscellaneous publication, no 30. Part III—Odisha, pp 45–46
Ghosh R, Baidya TK (2017) Using BIF magnetite of the Badampahar greenstone belt, Iron Ore Group, East Indian Shield to reconstruct the water chemistry of a 3.3–3.1 Ga sea during iron oxyhydroxides precipitation. Precambr Res 301:102–112
Ghosh S, De S, Mukhopadhyay J (2016) Provenance of 12.8 Ga Keonjhar Quartzite, Singhbhum Craton, Eastern India: implications for the nature of Mesoarchean upper crust and geodynamics. J Geol 124:331–351
Ghosh R, Vermeesch P, Gain D, Mondal R (2019) Genetic relationship among komatiites and associated basalts in the Badampahar greenstone belt (3.25–3.10 Ga), Singhbhum Craton. Eastern India Precambrian Res 327:196–211
Gudelius D, Zeh A, Wilson AH (2020) Zircon formation in mafic and felsic rocks of the Bushveld Complex (South Africa): constraints from composition, zoning, Th/U ratios, morphology, and modelling. Chem Geol 546:119647
Haque MW, Dutta SK (1996) Report on the investigation of gold in Dhanjori Basin in East Singhbhum district, Bihar. Progress Report for field season 1995–96. Geological Survey of India, Kolkata
Heinrich CA (2015) Witwatersrand gold deposits formed by volcanic rain, anoxic rivers and Archaean life. Nat Geosci 8:206–209
Hofmann A, Mazumder R (2015) A review of the current status of the Older Metamorphic Group and Older Metamorphic Tonalite Gneiss: insights into the Palaeoarchaean history of the Singhbhum craton, India. Memoirs Geol Soc Lond 43:103–107
Horscroft FDM, Mossman DJ, Reimer TO, Hennigh Q (2011) Witwatersrand metallogenesis: the case for (modified) syngenesis. SEPM Special Publication 101:75–95
Jodder J, Hofmann A, Ueckermann H (2021) 3.51 Sa old felsic volcanic rocks and carbonaceous cherts from the Gorumahisani greenstone belt insights into the Palaeoarchaean record of the Singhbhum Craton India. Precambrian Res 357:106109
Kirkland CL, Smithies RH, Taylor RJM, Evans N, McDonald B (2015) Zircon Th/U ratios in magmatic environs. Lithos 212–215:397–414
Koglin N, Zeh A, Frimmel HE, Gerdes A (2010) New constraints on the auriferous Witwatersrand sediment provenance from combined detrital zircon U-Pb and Lu-Hf isotope data for the Eldorado Reef (Central Rand Group, South Africa). Precambr Res 183:817–824
Kumar A, Venkatesh AS, Kumar P, Rai AK, Parihar PS (2017) Geochemistry of Archean radioactive quartz pebble conglomerates and quartzites from western margin of Singhbhum-Orissa Craton, eastern India: implications on paleo-weathering, provenance and tectonic setting. Ore Geol Rev 89:390–406
Liu Y, Gao S, Hu Z, Zong CGK, Wang D (2010) Continental and oceanic crust recycling-induced melt-peridotite interactions in theTrans-North China Orogen: U-Pb dating, Hf isotopes and trace elements in zircons from mantle xenoliths. J Petrol 51:537–571
Liu H, Zartman RE, Ireland TR, Sun WD (2019) Global atmospheric oxygen variations recorded by Th/U systematics of igneous rocks. Proc Natl Acad Sci 116:18854–18859

Ludwig KR (2003) Isoplot 3.00: a geochronological toolkit for Microsoft Excel. Berkeley Geochronology Center, Spec Publ 4, p 74
Luo G, Ono S, Beukes NJ, Wang DT, Xie S, Summons RE (2016) Rapid oxygenation of Earth's atmosphere 2.33 billion years ago. Sci Adv 2:e1600134
Luskin C, Wilson A, Gold D, Hofmann A (2019) The Pongola Supergroup: Mesoarchaean deposition following Kaapvaal Craton stabilization. In: Kröner A, Hofmann A (eds) The Archaean Geology of the Kaapvaal Craton. Southern Africa, Regional Geology Rev, Springer, Heidelberg, pp 225–254
Manikyamba C, Pahari A, Santosh M, Ray J, Sindhuja CS, Subramanyam KSV, Singh MR (2020) Mesoarchean gabbro-anorthosite complex from Singhbhum Craton. India Lithos 366–367:105541. https://doi.org/10.1016/j.lithos.2020.105541
Mazumder R, Chaudhuri T, Biswas S (2019) Palaeoarchean sedimentation and magmatic processes in the eastern Iron Ore Group, eastern India: a commentary. Geol J 54:3078–3087
Miller SR, Mueller PA, Meert JG, Kamenov GD, Pivarunas AF, Sinha AK, Pandit MK (2018) Detrital zircons reveal evidence of Hadean crust in the Singhbhum Craton, India. J Geol 126:541–552
Mitra A, Dey S, Kequing Z, Liu Y, Mitra A (2019) Building the core of a Paleoarchean continent: evidence from granitoids of Singhbhum Craton, eastern India. Precambr Res 335:105436
Mukhopadhyay D, Matin A (2020) The architecture and evolution of the Singhbhum Craton. Episodes 43:19–50
Mukhopadhyay J, Beukes NJ, Armstrong RA, Zimmermann U, Ghosh G, Medda RA (2008) Dating the oldest greenstone in India, a 3.51 Ga precise U-Pb SHRIMP zircon age for dacitic lava of the Southern Iron Ore Group. Singhbhum Craton the J Geol 116:449–461
Mukhopadhyay J, Crowley QG, Ghosh S, Ghosh G, Chakrabarti K, Misra B, Heron K, Bose S (2014) Oxygenation of the Archean atmosphere: new paleosol constraints from eastern India. Geology 42:923–926
Nelson D, Bhattacharya HN, Thern ER, Altermann W (2014) Geochemical and ion-microprobe U-Pb zircon constraints on the Archaean evolution of Singhbhum Craton, eastern India. Precambr Res 255:412–432
Nwaila G, Frimmel HE, Minter WEL (2017) Provenance and geochemical variations in shales of the Mesoarchaean Witwatersrand Supergroup. J Geol 125:399–422
Olierook HKH, Clark C, Reddy SM, Mazumder R, Jourdan F, Evan NJ (2019) Evolution of the Singhbhum Craton and supracrustal provinces from age, isotopic and chemical constraints. Earth-Sci Rev 193:237–259
Paprika D, Hofmann A, Agangi A, Elburg M, Xie H, Hartmann S (2021) Age of the Dominion-Nsuze Igneous Province, the first intracratonic Igneous Province of the Kaapvaal Craton. Precambr Res 363:106335
Planavsky N, Asael D, Hofmann A, Reinhard CT, Lalonde SV, Knudsen A, Wang X, Ossa Ossa F, Pecoits E, Smith B, Beukes N, Bekker A, Konhauser KO, Johnson TM, Lyons TW, Rouxel OJ (2014) Evidence for oxygenic photosynthesis half a billion years before the Great Oxidation Event. Nat Geosci 7:283–286
Prakash Pandey O, Mezger K, Ranjan S, Upadhyay D, Villa IM, Nägler TF, Vollstaedt H (2019) Genesis of the Singhbhum Craton, eastern India; implications for Archean crust-mantle evolution of the Earth. Chem Geol 512:85–106
Prabhakar N, Bhattacharya A (2013) Paleoarchean partial convective overturn in the Singhbhum Craton, Eastern India. Precambrian Res 231:106–121
Rao VM, Sinha KK, Mishra B, Balachandran K, Srinivasan S, Rajasekharan P (1988) Quartz-pebble conglomerate from the Dhanjori—a new uranium horizon of Singhbhum uranium province. J Geol Soc India 9:89–95
Roy AB, Bhattacharya HN (2012) Tectonostratigraphic and geochronologic reappraisal constraining the growth and evolution of Singhbhum Archaean Craton, Eastern India. J Geol Soc India 80:455–469
Rudnick RL, Gao S (2005) Composition of the continental crust. In: Rudnick RL (ed) The Crust. Elsevier, Amsterdam, pp 1–64
Saha AK (1994) Crustal evolution of Singhbhum-North Orissa, eastern India. Memoirs Geol Soc India 27:341p
Saha D, Bacchar P, Deb GK, Patranabis-Deb S, Banerjee A (2021) Tectonic evolution of the Paleoarchean to Mesoarchean Badampahar-Gorumahisani belt, Singhbhum craton, India implications for coexisting arc and plume signatures in a granite-greenstone terrain. Precambr Res 357:106094. https://doi.org/10.1016/j.precamres.2021.106094
Sarangi BB, Mohanty A (1987) A report on the preliminary investigation for gold and heavy metals in Badampahar-Suleipat area. Geological Society of India, company report, Mayurbhanja district, Orissa, pp 85–86
Scherer E, Münker C, Metzger K (2001) Calibration of the lutetium-hafnium clock. Science 293:683–687
Sreenivas B, Dey S, Rao YB, Kumar TV, Babu E, Williams IS (2019) A new cache of Eoarchaean detrital zircons from the Singhbhum craton, eastern India and constraints on early Earth geodynamics. Geosci Front 10:1359–1370
Sunilkumar T, Parthasarathy R, Palrecha M, Shah V, Sinha K, Krishna Rao N (1996) Chemical age of detrital zircons from the basal quartz-pebble conglomerate of Dhanjori Group, Singbhum craton, Eastern India. Curr Sci 71:482–486
Upadhyay D, Chattopadhyay S, Kooijman E, Mezger K, Berndt J (2014) Magmatic and metamorphic history of Paleoarchean tonalite-trondhjemitegranodiorite (TTG) suites from the Singhbhum craton, eastern India. Precambr Res 252:180–190
Vermeesch P (2012) On the visualization of detrital age distributions. Chem Geol 312–313:190–194
Wiedenbeck M, Allé P, Corfu F, Griffin WL, Meier M, Oberli F, von Quadt A, Roddick JC, Spiegel W (1995) Three natural zircon standards for U-Th-Pb, Lu-Hf, trace element and REE analyses. Geostand Newsl 19:1–23
Wilson AH, Zeh A (2018) U-Pb and Hf isotopes of detrital zircons from the Pongola Supergroup: constraints on deposition ages, provenance and Archaean evolution of the Kaapvaal Craton. Precambr Res 305:117–196
Woodhead JD, Hergt JM (2005) A preliminary appraisal of seven natural zircon reference materials for *in situ* Hf isotope determination. Geostand Geoanal Res 29:183–195
Yadav PK, Das M (2021) Geochemistry of metasedimentary clastic rocks from Dhanjori and Badampahar Groups, Singhbhum Craton, Eastern India: implications for tectonic setting and Archean-Proterozoic boundary. J Sediment Environ 6:447–472
Zeh A, Wilson AH (2022) U-Pb-Hf isotopes and shape parameters of zircon from the Mozaan Group (South Africa) with implications for depositional ages, provenance and Witwatersrand – Pongola Supergroup correlations. Precambr Res 368:106500
Zeh A, Gerdes A, Will TM, Frimmel H (2010) Hafnium isotope homogenization during metamorphic zircon growth in amphibolite-facies rocks, examples from the Shackleton Range (Antarctica). Geochim Cosmochim Acta 74:4740–4758
Zeh A, Gerdes A, Barton JM Jr, Klemd R (2010) U-Th-Pb and Lu-Hf systematics of zircon from TTG's, leucosomes, anorthosites and quartzites of the Limpopo Belt (South Africa): constraints for the formation, recycling, and metamorphism of Paleoarchean crust. Precambr Res 179:50–68